

A novel mechatronic system for evaluating elbow muscular spasticity relying on Tonic Stretch Reflex Threshold estimation

*Original*

A novel mechatronic system for evaluating elbow muscular spasticity relying on Tonic Stretch Reflex Threshold estimation / Averta, G.; Abbinante, M.; Orsini, P.; Felici, F.; Lippi, P.; Bicchi, A.; Catalano, M. G.; Bianchi, M.. - (2020), pp. 3839-3843. (Intervento presentato al convegno 42nd Annual International Conferences of the IEEE Engineering in Medicine and Biology Society, EMBC 2020 tenutosi a can nel 2020) [10.1109/EMBC44109.2020.9176011].

*Availability:*

This version is available at: 11583/2970277 since: 2022-09-02T09:13:20Z

*Publisher:*

Institute of Electrical and Electronics Engineers

*Published*

DOI:10.1109/EMBC44109.2020.9176011

*Terms of use:*

This article is made available under terms and conditions as specified in the corresponding bibliographic description in the repository

*Publisher copyright*

IEEE postprint/Author's Accepted Manuscript

©2020 IEEE. Personal use of this material is permitted. Permission from IEEE must be obtained for all other uses, in any current or future media, including reprinting/republishing this material for advertising or promotional purposes, creating new collecting works, for resale or lists, or reuse of any copyrighted component of this work in other works.

(Article begins on next page)

# A novel mechatronic system for evaluating elbow muscular spasticity relying on Tonic Stretch Reflex Threshold estimation

Giuseppe Averta<sup>1,2,3</sup>, Massimiliano Abbinante<sup>1</sup>, Piero Orsini<sup>1</sup>, Federica Felici<sup>2</sup>, Paolo Lippi<sup>4</sup>, Antonio Bicchi<sup>1,2,3</sup>, Manuel G. Catalano<sup>1,2</sup>, and Matteo Bianchi<sup>1,3</sup>

**Abstract**—Muscular spasticity represents one of the most common motor disorder associated to lesions of the Central Nervous System, such as Stroke, and affects joint mobility up to the complete prevention of skeletal muscle voluntary control. Its clinical evaluation is hence of fundamental relevance for an effective rehabilitation of the affected subjects. Standard assessment protocols are usually manually performed by humans, and hence their reliability strongly depends on the capabilities of the clinical operator performing the procedures. To overcome this limitation, one solution is the usage of mechatronic devices based on the estimation of the Tonic Stretch Reflex Threshold, which allows for a quite reliable and operator-independent evaluation. In this work, we present the design and characterization of a novel mechatronic device that targets the estimation of the Tonic Stretch Reflex Threshold at the elbow level, and, at the same time, it can potentially act as a rehabilitative system. Our device can deliver controllable torque/velocity stimulation and record functional parameters of the musculo-skeletal system (joint position, torque, and multi-channel ElectroMyoGraphyc patterns), with the ultimate goals of: i) providing significant information for the diagnosis and the classification of muscular spasticity, ii) enhancing the recovery evaluation of patients undergoing through therapeutic rehabilitation procedures and iii) enabling a future active usage of this device also as therapeutic tool.

**Clinical relevance**— The contribution presented in this work proposes a technological advancement for a device-based evaluation of motion impairment related to spasticity, with a major potential impact on both the clinical appraisal and the rehabilitation procedures.

## I. INTRODUCTION AND MOTIVATION

The connective-musculo-skeletal system is a marvelous and extremely complex natural system, organized in rigid segments (bones) that are moved by a redundant number of muscles through specific connective structures (tendons, aponeuroses, etc.). In physiological conditions, this system is responsible for the extraordinary adaptability in motion execution. When a lesion affects the Central Nervous System (CNS), e.g. stroke, stereotyped movement patterns arise, which are the consequence of the pathological coupling between different Degrees of Freedom (DoFs) and of the loss of individual control over single joints [1]. This behavior can be observed both at the level of the upper limb, during reaching and task-oriented movements, and at the level of the lower limb, during gait.

Among the different neurological diseases, stroke has a considerable societal impact and represents one of the main causes of death and disability worldwide. For example,

<sup>1</sup> Centro di Ricerca “Enrico Piaggio”, Università di Pisa, Pisa, Italy giuseppe.averta@ing.unipi.it <sup>2</sup> Soft Robotics for Human Cooperation and Rehabilitation, Fondazione Istituto Italiano di Tecnologia Genova, Italy. <sup>3</sup> Dipartimento di Ingegneria dell’Informazione, Università di Pisa, Pisa, Italy. <sup>4</sup> University of Florence, Florence, Italy



Fig. 1: Overview of the proposed device while a subject is performing the task.

looking at the United States only, an American dies of stroke every 4 min (Centers for Disease Control and Prevention, 2015). In stroke patients, it is common to observe an impairment of the sensory-motor capabilities, which is typically associated to the reduction of the active range of motion, the loss of meaningful inter-joint coordination, muscle weakness and spasticity [2], [3], [4].

Spasticity is characterized by an involuntary velocity-dependent stretch reflex that causes inappropriate activation of the stretched muscle during passive and active movements. This leads to the abnormal increase of the resistance to the motion itself, as underlined in the classical definition of Lance [5]. It is hence clear that the clinical appraisal of muscle spasticity is highly relevant not only for the assessment of the level of impairment but also to evaluate the effects of the rehabilitation strategies in use.

To this aim, standard clinical approaches often rely on the application of a modified Ashworth scale (MAS) [6], which quantifies the resistance exhibited by a muscle that undergoes through passive movements imposed by the examiner. However, since muscle stretch resistance is a combination of multiple causes, which act both at the central neural level and locally (due to the modification of the viscoelastic properties of muscles, tendons and ligaments), MAS cannot distinguish between the neural and non-neural components. Furthermore, the MAS scale is not able to evaluate the velocity-dependent resistance to passive stretching, which is one of the core characteristics of spasticity. Last but not least, MAS evaluation is highly operator-dependent, since it is usually manually performed.

To overcome these limitations, alternative approaches based on the equilibrium point hypothesis (EPH) have been proposed [7], [8], [9], [10]. These methodologies leverage

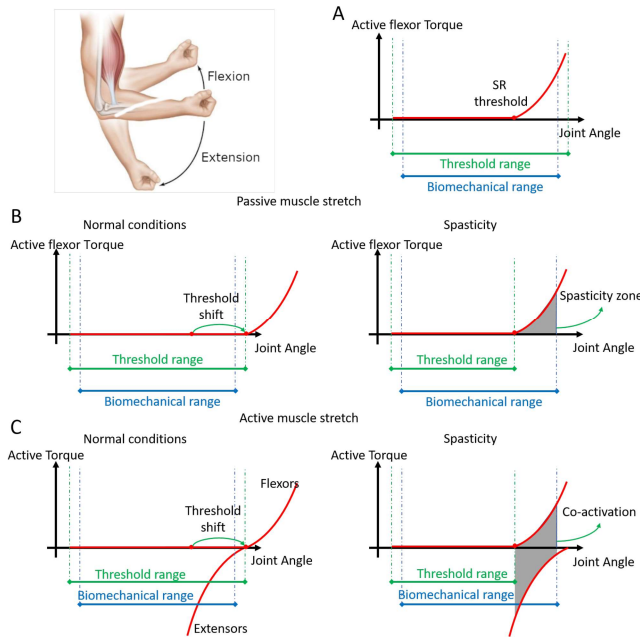


Fig. 2: Schematics of elbow movements in passive and active conditions. A) Nominal conditions in steady state; B) Passive extension of the elbow in normal and pathological conditions. The latter case shows the torque actively generated by the flexor muscle over joint angles, during spasticity of the flexor muscle; C) Active extension of the elbow in normal and pathological conditions. The latter case shows a co-activation pattern, required to overcome the resistance to motion of flexor muscles due to spasticity.

on the estimation of the Tonic Stretch Reflex Threshold (TSRT) for the evaluation of neural-related motor impairment. Furthermore, the application of EPH to stroke patient rehabilitation was proven to produce promising results in terms of an increase in muscular recruitment [11]. Under this regard, it is worth mentioning the *Grimaldi's method* [12]. This therapeutic maneuver specifically acts on TSRT of a selected muscular group, which is shortened in a passive way by applying a series of fast accelerations, while the limb, bound by a mechanical system, is being moved by forces applied in the opposite direction.

It is hence clear that the correct estimation of the TSRT is of paramount importance not only for diagnostic but also for therapeutic purposes. This estimation usually relies on the usage of a mechatronic device – thus minimizing the dependence of the evaluation outcomes on the manual capabilities of the operator. The device applies a controllable torque that is co-axial to the joint under investigation, and record joint angular position and surface ElectroMyoGraphyc (EMG) patterns, e.g. at the elbow level in the adults [13], [14], and the ankle level in children with muscular spasticity associated to cerebral palsy [9].

However, the development of this kind of systems for the upper limb is not a trivial problem, since it comes with very strict requirements, which are mainly related to the need for: i) a portable design, to enable the usage in clinical environments; ii) different regulation and control possibilities to accommodate various pathological conditions, with special focus on shoulder abduction and flexion, and wrist flexion-extension; iii) a reduced active interaction between patients and therapists during the evaluation task.

In this paper, we present the design and characterization of a new mechatronic device, depicted in Fig. 1, which targets

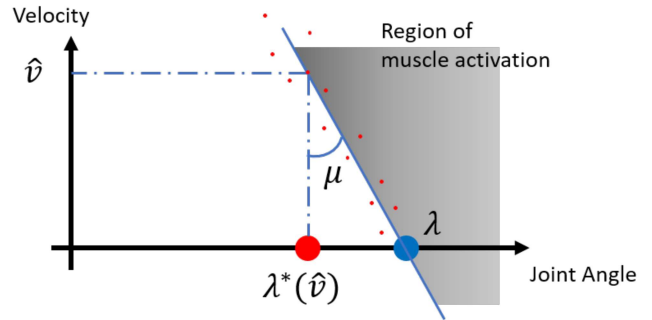


Fig. 3: Linear regression of multiple DSRT measurements used to estimate the TSRT. The angular value  $\lambda^*(\hat{v})$  at which the muscle begins to be activated is measured considering different peak velocities  $\hat{v}$  (red dots). A linear regression (blue line, with  $\mu$  coefficient of the linear approximation) is then used to estimate the value of  $\lambda$  in static conditions (i.e.  $v \approx 0$ ).

the estimation of the TSRT in adult subjects at the elbow level, where spasticity is preminent and present in the 79% of stroke cases [15]. This system was thought to correctly satisfy the aforementioned requirements and apply torque-velocity stimuli, which are coherent with the dedicated literature. It is also worth noticing that the fulfilment of the latter ones for the TSRT estimation phase also enables the possible usage of this device as an active therapeutic tool based on [12]. To conclude, although a clinical validation still lacks and is needed, the system described in this preliminary work potentially represents the first technology that allows for both the measurement and rehabilitation of TSRT in patients affected by muscular spasticity.

## II. SPASTICITY AND EQUILIBRIUM POINT HYPOTHESIS

Introduced by A. Feldman, the equilibrium point hypothesis (EPH) is an interesting yet debated theory in motor control [16], [17], [18]. In a nutshell, the idea is that the CNS does not directly control the activation of all body muscles, but rather is able to modify the stretch-reflex (SR) threshold, defined as the spatial value of muscle length at which a given muscle begins to be activated, if stretched at a given stretch velocity.

For a given coordinated set of thresholds, the system results in a stable equilibrium between internal visco-elastic forces and external loads, and movements are generated through a time-dependent coherent modification of these equilibrium points. In physiological conditions, the SR threshold can be arbitrarily "set" by the CNS to any value within and beyond the range of angular variation in the joint considered. Therefore, the central adjustment range of the control variables (muscle SR thresholds) exceeds the biomechanical range of angular variation in a joint.

On the contrary, it has been suggested that some CNS injuries may result in a reduction of the admitted range of variability of the SR threshold, which can be also observed considering the torque/angle plot for the analyzed joint, i.e. the maximum torque that the joint is able to actively resist at a given angular value [14]. This behavior can justify the occurrence of muscular spasticity (see Fig. 2).

This concept is supported by several experimental findings (see e.g. [19], [13], [14]), in which authors reported on changes of the SR thresholds for both flexor and extensor muscular groups at the elbow level, in subjects affected by stroke or cerebral palsy. In these cases, threshold values

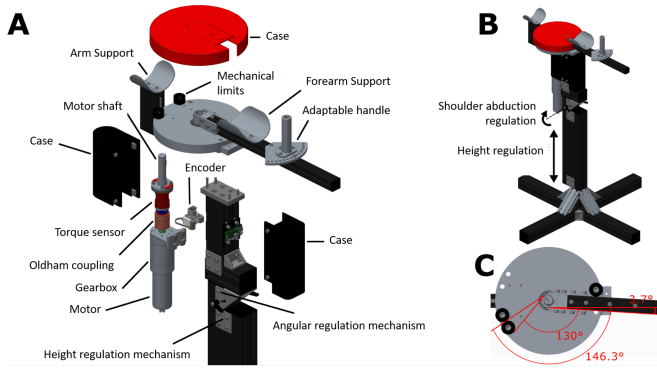


Fig. 4: Mechanical design of the proposed device. A) Exploded view; B) Full view, with details on possible regulations to adapt the device to the user; C) Top view, with details on mechanical limit bumpers and joint range-of-motion. The device can be mounted as to be used with both arms, in C) the components are mounted targeting the usage with the left arm.

are reduced within the biomechanical joint nominal range. Similar results were also discussed at the ankle level in adult patients after stroke [20], and in children with cerebral palsy [9]. The SR thresholds discussed so far are intended in static conditions and typically named with the symbol  $\lambda$  - also referred to as *Tonic Stretch Reflex Threshold* (TSRT). It is, however, worth mentioning that the real behavior of SR depends on the stretch velocity ( $v$ ), and is described as *Dynamic Stretch Reflex Threshold* (DSRT)  $\lambda^*(v)$ , whose relation with the TSRT can be linearly approximated as  $\lambda^*(v) = \lambda - \mu v$ . Due to the extreme difficulty in directly measuring the TSRT, its value is then typically estimated from a series of observation of the DSRT. The joint is passively stretched using bell-shaped velocity profiles with different peak values and, for each trial velocity peak  $\hat{v}$ , the examiner records the joint angular value  $\lambda^*(\hat{v})$  at which the muscle begins to be activated. Hereinafter we refer to this stimulation to as mode A (see Section IV). A linear regression is then used to estimate the static value of  $\lambda$  (see Fig. 3).

To quantify pathological conditions based on EHP, we then propose a device that can i) precisely implement mode A stimulation and apply a torque co-axially with the examined joint (in our case the elbow flexion-extension) for retrieving the torque/angle characteristics (mode B) in agreement with [14], ii) enable synchronous software recording of the actual joint angles, torques and the surface EMG patterns of specific muscles (flexors and extensors), and iii) potentially acts as an active therapeutic tool implementing the maneuver in [12].

### III. MECHANICAL DESIGN

The proposed device consists of two rigid segments, one supporting the upper arm and the second supporting the forearm (see Fig. 5-E,F for a full view). These are mounted on a support platform that grounds the whole structure on the floor and whose height can be adapted for different subjects' heights (from 145 to 210 cm) by maneuvering a passive prismatic joint (see Fig. 4-B). The forearm support is actuated through a DC motor, mounted with the axis along the main axis of the elbow flexion-extension DoF and coupled with a torque sensor. An encoder is also included to measure joint angular values, together with torque and surface EMG sensors. The whole system is intended to be used by a subject seating on an adjustable chair, to accommodate for different

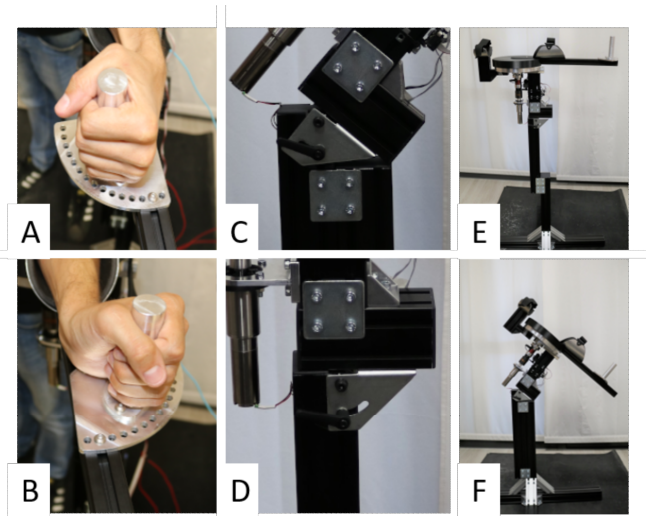


Fig. 5: Details of the proposed device. In Subfigs A,B regulations of the wrist flexion-extension. In Subfigs C,D linear and angular regulations at the shoulder level. In subfigs E,F full view of the proposed design in two different configurations.

subject body dimensions and pathological conditions. The total device weight is less than 20 Kg. A detailed exploded view is reported in Fig. 4-A.

The elbow can rotate (actively or passively) around the motor axis in the range  $[34^\circ, 176^\circ]$ , considering a safety margin of  $4^\circ$  w.r.t. the nominal elbow range [21] (see Fig. 4-C). The elbow total movement can be also mechanically limited to the range  $[50^\circ, 176^\circ]$ , through the usage of mechanic bumpers, for patients in which the wrist is completely flexed due to spasticity (see Fig. 4-C for details). Shoulder abduction can be manually regulated through a passive revolute joint mechanism in the range  $[65^\circ, 90^\circ]$  (see Fig. 5-C,D and Fig. 4-B), while hand support inclination w.r.t. the forearm (around the flexion-extension axis) can be mounted in multiple configurations (regulation step of  $5^\circ$  in the range  $[0^\circ, 60^\circ]$ ) through the adaptable handle shown in Fig. 5-A,B. The handle can also slide along the forearm main axis to account for different forearm lengths, with a distance between handle and motor axis ranging between 29 and 42 cm. All the regulation ranges were designed considering average biomechanical dimensions (see [21]).

To identify the minimum motor characteristics, we considered the requirements of the two experimental conditions: TSRT estimation and torque/angle diagram estimation [14]. During the first experimental condition, the subject is asked to keep the arm relaxed while a velocity profile is applied. Assuming that we can neglect the dynamics after the SR (not relevant for the analysis), we considered a required maximum peak velocity equal to  $300^\circ/\text{s}$ , to be applied for 1.2 s (see [22], equivalent to 50 rpm). Considering the second experimental condition, instead, the maximum velocity required is  $8^\circ/\text{s}$ , to be applied for less than 30 s. The maximum torque considered is derived by the experiments discussed in [14] (40 Nm) and over-respected with a design limit set to 60 Nm.

To satisfy all these requirements, we selected a 24V DC brushed motor (Maxon Motors, mod RE50), coupled with a gearbox with a reduction factor equal to 71 : 1 (Maxon Motors, mod GP62). This system is able to perform a

maximum peak velocity equal to 63 rpm and a maximum torque equal to 63.9 Nm, thus satisfying the design specifics. Motor and gearbox are coupled through a Oldham coupling (mod MOM-38K from NBM, maximum torque 110 Nm, maximum velocity 2000 rpm). The torque sensor used is the TFF-350-FSH04063 by Futek, with full-scale equal to 150 Nm, maximum measure error equal to 0.45 Nm and dimensions comparable with those of the motor. The encoder used is an Austrian Microsystems AS5045 (12 bit, resolution 0.0875°). The electronic board, together with the software and libraries used in the proposed device are extracted from Natural Machine Motion Initiative<sup>1</sup> (NMMI) platform. The microcontroller CY8C3246PVI-147 48-SSOP from PSoC is embedded in the control board, connected to a PC via USB. MATLAB/Simulink libraries are used to control the motor, record force, velocity data and EMG signals (in our case we consider the 4 electrodes by Ottobock. Note, however, that this architecture is modular) a 1 KHz loop.

#### A. Evaluation of Mechanical Strength

Due to the high forces involved during the usage of the device, we performed mechanical strength evaluation of all the components included in the design. Aluminium bars used to support arm and forearm were analysed using a beam model, while the other connection components were analysed using a Finite Element Modeling (FEM) analysis using the software PTC Creo Engineer.

1) *Frame*: The frame is made by aluminium bars, with a yielding stress of 205 Mpa. Considering the forearm support, the critical section is at the connection between the bar and the pulley of the crankshaft. The equivalent Tresca stress is 41.7 Mpa, then with a safety coefficient  $\eta = 4.9$ . Regarding the upper arm support bar, the critical section is at the coupling with the base support, with a critical condition for maximum extension of the bar. In this case, the equivalent Tresca stress is 47.9 Mpa, then with a safety coefficient  $\eta = 4.3$ .

2) *Crankshaft*: The crankshaft is made in aluminium 7075-T6 (UNI EN 573-3), supporting up to 434 Mpa and with a Young module of 71 Gpa. In its critical section (higher bearing) the equivalent Tresca stress is 114.7 Mpa, safety coefficient  $\eta = 3.75$ . For deformation evaluation, we used the Mohr method and verified that at the joint level the angular and radial deformations are negligible w.r.t. to the margin admitted by the Oldham coupling.

3) *Bearings*: Radial loads on the higher and lower bearings are 2.79 kN and 2.37 kN respectively, while axial loads are negligible. Radial static load coefficient is 4.4 kN, then the safety coefficient is equal to  $\eta = 1.58$ .

#### IV. CONTROL

The two evaluation procedures discussed above require two different control strategies: a position control for the estimation of the TSRT (mode A), and a torque regulation for the estimation of the torque/angle plot (mode B). Both the controllers were developed in Matlab Simulink to enable a fast prototyping and easy tuning of parameters. The input considered is the tension applied to the motor (PWM), while

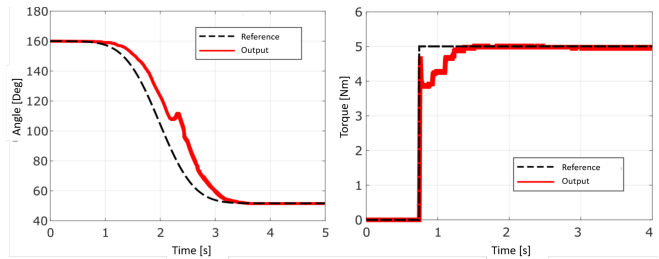


Fig. 6: On the left, reference and output during a test with position control and an external disturbance due to muscle contraction. Peak velocity was equal to 90°/s. On the right, reference and output during a test in torque control for the estimation of torque/angle plot.

the output is the position of the motor (mode A) or the applied torque (mode B).

a) *Mode A: Position Control*: To precisely regulate the angular position of the motor, we implemented a PID controller  $C(s) = K_c(1 + \frac{1}{\tau_i s} + \tau_d s) \frac{1}{1 + \tau_p s}$ . Parameters were tuned following a the closed-loop Ziegler-Nichols rule with no overshoot. Tuned parameters of the controller were  $K_c = 0.64$ ,  $\tau_i = 0.19$ ,  $\tau_d = 0.125$  and  $\tau_p = \frac{1}{300}$ .

b) *Mode B: Torque Control*: To control the torque we used a PI regulator  $C(s) = K_c(1 + \frac{1}{\tau_i s})$ , tuned through the Frequency-Response Based Tuning available in Matlab. Design requirements included a step response lower than 0.3s with no overshoot, a bandpass of 10°/s and a phase margin of 90°. Tuned parameters were  $K_c = 0.3$  and  $\tau_i = 0.025$ .

#### V. PRELIMINARY EXPERIMENTS WITH HEALTHY SUBJECT

To test the performance of our device, and its control, during usage in both the experimental conditions (mode A and B), we performed a set of experiments with one healthy participant (right-handed, M. 27).

Preliminary tests in mode A (see Fig. 7) were performed by commanding trajectories with bell shaped velocity profiles (peak velocity ranging between 10°/s and 110°/s) (the upper limit is chosen for safety reasons) with a load on the arm and forearm supports equal to 1.7 and 3 Kg respectively, coherently with [21]. Maximum tracking error recorded was lower than 1°. Then, a simulation of the experiment for the estimation of the TSRT was performed. A naive subject was asked to hold the handle - whose configuration was carefully adapted to his specific body dimensions - and to keep upper limb muscles relaxed. Then, bell-shaped velocity profiles were applied to the motor considering the peak values in the range from 10°/s to 110°/s. Subject was asked to contract the muscles in the middle of the trajectory (close to the velocity peak, to simulate the stretch reflex). Performance of the controller during these tests were collected and analysed by recording commanded and real position of the forearm support. In Fig. 6-left we show the outcome of these experiments for the case of 90°/s. It is possible to observe a prompt and smooth response of the controller to the external disturbance caused by the subject muscular contraction.

Tests in mode B were first performed with the axis of the motor parallel to the floor and with a weight at the extremity of the forearm support equal to 5 Kg (i.e. a pendulum configuration). Experiments were conducted by evaluating the step response, considering input reference torques ranging between 1 and 10 Nm. Maximum steady state error

<sup>1</sup><https://www.naturalmachinemotioninitiative.com/>

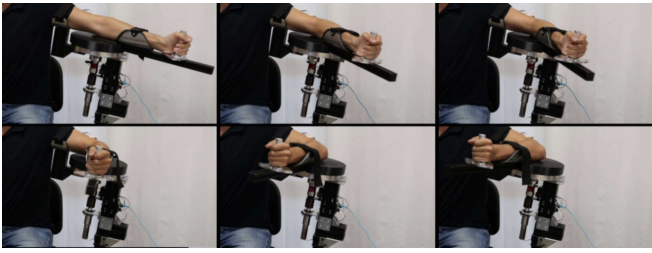


Fig. 7: Snapshot of a test simulating the estimation of the TSRT (mode A), performed using the device presented in this paper. Subject was asked to grasp the handle and keep the arm muscles relaxed. Then, a bell-shaped velocity profile was applied to the motor imposing a passive motion to the subject forearm.

recorded was always lower than 0.3Nm. Then, a simulation of the experiment for the estimation of the torque/angle plot was performed. The subject was asked to slowly move the arm in flexion (average velocity  $10^\circ/\text{s}$ ) multiple time. The first repetition was performed in free motion, then at each iteration the opposite torque was increased of 1 Nm, up to the threshold of 10 Nm. The measured and commanded torque value for the case of opposite torque equal to 5 Nm is reported in Fig. 6-right. Note that the time-to-rise of the step response is mainly related to the muscle response time.

## VI. CONCLUSIONS

In this paper we presented a new mechatronic device to be used for the diagnosis and the evaluation of spasticity phenomena at the elbow level. Moving from current state-of-the-art devices and clinical specifications, we proposed a new implementation that is portable and enable different regulations and control possibilities, opening the possibility to minimize the active interaction between patients and therapists during the evaluation task, thus the operator-dependent effects. It is also worth mentioning that our design could be potentially used as an active therapeutic tool based on the maneuver presented in [12], and the evaluation of recovery could be also associated with functional-based approaches that quantify the quality of movement in activities of daily living [23], [24]. Preliminary experiments with one healthy participant demonstrated that our device is able to replicate both the experimental procedures envisioned (mode A and B) with good performance in terms of tracking errors. A careful and extended experimental campaign with healthy and stroke-affected subjects is currently under evaluation and is left for future developments of this work.

## ACKNOWLEDGMENT

This project received funding from the European Union's Horizon 2020 research and innovation programme under grant agreement No. 688857 (SoftPro).

## REFERENCES

- [1] M. Santello and C. E. Lang, "Are movement disorders and sensorimotor injuries pathologic synergies? when normal multi-joint movement synergies become pathologic," *Frontiers in human neuroscience*, vol. 8, p. 1050, 2015.
- [2] D. Bourbonnais and S. V. Noven, "Weakness in patients with hemiparesis," *American Journal of Occupational Therapy*, vol. 43, no. 5, pp. 313–319, 1989.
- [3] D. K. Sommerfeld, E. U.-B. Eek, A.-K. Svensson, L. W. Holmqvist, and M. H. von Arbin, "Spasticity after stroke: its occurrence and association with motor impairments and activity limitations," *Stroke*, vol. 35, no. 1, pp. 134–139, 2004.

- [4] M. F. Levin, "Interjoint coordination during pointing movements is disrupted in spastic hemiparesis," *Brain*, vol. 119, no. 1, pp. 281–293, 1996.
- [5] R. G. Feldman, R. R. Young, and W. P. Koella, "Spasticity: disordered motor control." Symposia Specialists, Incorporated, 1980.
- [6] C. P. Charalambous, "Interrater reliability of a modified ashworth scale of muscle spasticity," in *Classic papers in orthopaedics*. Springer, 2014, pp. 415–417.
- [7] A. Calota, A. G. Feldman, and M. F. Levin, "Spasticity measurement based on tonic stretch reflex threshold in stroke using a portable device," *Clinical Neurophysiology*, vol. 119, no. 10, pp. 2329–2337, 2008.
- [8] A. Calota and M. F. Levin, "Tonic stretch reflex threshold as a measure of spasticity: implications for clinical practice," *Topics in stroke rehabilitation*, vol. 16, no. 3, pp. 177–188, 2009.
- [9] M. Germanotta, J. Taborri, S. Rossi, F. Frascarelli, E. Palermo, P. Cappa, E. Castelli, and M. Petrarca, "Spasticity measurement based on tonic stretch reflex threshold in children with cerebral palsy using the pedianklebot," *Frontiers in human neuroscience*, vol. 11, p. 277, 2017.
- [10] I. A. Marques, M. B. Silva, A. N. Silva, L. M. D. Luiz, A. B. Soares, and E. L. M. Naves, "Measurement of post-stroke spasticity based on tonic stretch reflex threshold: implications of stretch velocity for clinical practice," *Disability and rehabilitation*, vol. 41, no. 2, pp. 219–225, 2019.
- [11] A. Crippa, R. Cardini, D. Pellegatta, S. Manzoni, D. Cattaneo, and F. Marazzini, "Effects of sudden, passive muscle shortening according to grimaldi's method on patients suffering from multiple sclerosis: a randomized controlled trial," *Neurorehabilitation and neural repair*, vol. 18, no. 1, pp. 47–52, 2004.
- [12] L. Grimaldi, P. Lippi, P. Marri, M. Fantozzi, and R. Bracci, "Revoking of absent motor components in cns lesions," *Giardini*, vol. 1-3, 1986–88.
- [13] M. F. Levin and A. G. Feldman, "The role of stretch reflex threshold regulation in normal and impaired motor control," *Brain research*, vol. 657, no. 1-2, pp. 23–30, 1994.
- [14] M. F. Levin, R. W. Selles, M. H. Verheul, and O. G. Meijer, "Deficits in the coordination of agonist and antagonist muscles in stroke patients: implications for normal motor control," *Brain research*, vol. 853, no. 2, pp. 352–369, 2000.
- [15] J. Wissel, L. D. Schelosky, J. Scott, W. Christe, J. H. Faiss, and J. Mueller, "Early development of spasticity following stroke: a prospective, observational trial," *Journal of neurology*, vol. 257, no. 7, pp. 1067–1072, 2010.
- [16] A. G. Feldman, "Functional tuning of the nervous system with control of movement or maintenance of a steady posture-ii. controllable parameters of the muscle," *Biofizika*, vol. 11, pp. 565–578, 1966.
- [17] —, "Referent control of action and perception," *Challenging Conventional Theories in Behavioral Neuroscience*, 2015.
- [18] —, "Once more on the equilibrium-point hypothesis ( $\lambda$  model) for motor control," *Journal of motor behavior*, vol. 18, no. 1, pp. 17–54, 1986.
- [19] A. Jobin and M. F. Levin, "Regulation of stretch reflex threshold in elbow flexors in children with cerebral palsy: a new measure of spasticity," *Developmental medicine and child neurology*, vol. 42, no. 8, pp. 531–540, 2000.
- [20] A. K. Blanchette, A. A. Mullick, K. Moïn-Darbari, and M. F. Levin, "Tonic stretch reflex threshold as a measure of ankle plantar-flexor spasticity after stroke," *Physical therapy*, vol. 96, no. 5, pp. 687–695, 2016.
- [21] W. T. Dempster and G. R. Gaughran, "Properties of body segments based on size and weight," *American journal of anatomy*, vol. 120, no. 1, pp. 33–54, 1967.
- [22] N. A. Turpin, A. G. Feldman, and M. F. Levin, "Stretch-reflex threshold modulation during active elbow movements in post-stroke survivors with spasticity," *Clinical Neurophysiology*, vol. 128, no. 10, pp. 1891–1897, 2017.
- [23] G. Averta, C. Della Santina, G. Valenza, M. Bianchi, and A. Bicchi, "Exploiting upper-limb functional synergies for human-like motion generation of anthropomorphic robots," *Journal of NeuroEngineering and Rehabilitation*.
- [24] A. Schwarz, G. Averta, J. M. Veerbeek, A. R. Luft, J. P. Held, G. Valenza, A. Biechi, and M. Bianchi, "A functional analysis-based approach to quantify upper limb impairment level in chronic stroke patients: A pilot study," in *2019 41st Annual International Conference of the IEEE Engineering in Medicine and Biology Society (EMBC)*. IEEE, 2019, pp. 4198–4204.